

Impact of parity violation on quantum entanglement and Bell nonlocality

Yong Du,^{1,*} Xiao-Gang He,^{1,2,†} Chia-Wei Liu,^{1,‡} and Jian-Ping Ma^{3,4,5,§}

¹*Tsung-Dao Lee Institute, Shanghai Jiao Tong University, Shanghai 200240, China*

²*Key Laboratory for Particle Astrophysics and Cosmology (MOE)*

*Shanghai Key Laboratory for Particle Physics and Cosmology,
Shanghai Jiao Tong University, Shanghai 200240, China*

³*CAS Key Laboratory of Theoretical Physics, Institute of Theoretical Physics,*

P.O. Box 2735, Chinese Academy of Sciences, Beijing 100190, China

⁴*School of Physical Sciences, University of Chinese Academy of Sciences, Beijing 100049, China*

⁵*School of Physics and Center for High-Energy Physics, Peking University, Beijing 100871, China*

(Dated: October 31, 2024)

Quantum entanglement (QE), evidenced by Bell inequality (BI) violations, reveals the nonlocality of nature. Fundamental interactions manifest in various forms, each with distinct effects on QE and BI, but have not yet been studied in depth. We investigate in detail the relationship between QE, Bell nonlocality, and parity-violating interactions in spin-1/2 bipartite systems arising from the decays of spin-0 and spin-1 particles within the quantum field theory (QFT). Our findings reveal that parity (P) violation can completely disentangle particle pairs, rendering Bell tests ineffective in distinguishing between classical and quantum theories. In the spin-0 case, complete disentanglement occurs at maximal P violation, which is similarly true for spin-1 decays. Without restrictions from the QFT, the predicted relation between entanglement and the Bell nonlocality may no longer be valid and we propose promising methods for testing it. Additionally, we emphasize the previously overlooked influence of magnetic fields within detectors, which alters predictions for QE and Bell nonlocality. This environmental effect induces spurious P and charge-parity (CP) violations and thus has to be subtracted for genuine P, CP, and Bell tests.

Introduction.—Quantum entanglement (QE) is a fundamental property of quantum mechanics [1] that reveals the inherent nonlocality of nature, famously highlighted by violations of Bell inequalities (BI)[2]. These inequalities are satisfied by classical local hidden-variable theories but can be violated by quantum systems. Although parity (P) violation is an essential aspect of the Standard Model, current studies on QE and BI violations have mostly focused on P-conserving interactions [3–7], leaving the role of P violation in these contexts unclear up to now. In addition, many experimental tests of P and charge-parity (CP) violation rely on the presence of QE [8–10], yet neither QE nor BI violations have been fully examined in relation to such interactions.

In a broader context, the influence of fundamental particle interactions on the behavior of QE and BI violations has not been extensively investigated. These fundamental interactions manifest in various forms, even beyond the scope of classical and quantum theories, and they play a crucial role in shaping entanglement patterns as well as the degree of BI violations. Conversely, analyzing the characteristics of QE and BI can provide valuable insights into the nature of these underlying interactions.

We demonstrate these important features by studying P-violating interactions on QE and BI for spin-0 and spin-1 decays into two spin-1/2 particle systems in the quantum field theory (QFT). We find that QE and BI crucially depend on the degree of P violation. For P-conserving spin-0 decays, QE and BI violations are maximized, whereas P-violating interactions can completely disentangle bipartite systems, making Bell tests ineffec-

tive for distinguishing quantum from classical behavior. This finding holds similarly for spin-1 decays. We find simple ways to parameterize deviations from QFT which can be tested experimentally. Moreover, environmental factors like magnetic fields inside detectors can rotate particle spins and mimic P- and CP-violating effects. To accurately access QE and conduct genuine tests of BI, P, and CP violation, it is therefore crucial to account for these ontic environmental influences that were overlooked before in literature.

We start with a general discussion about QE and BI. The spin-1/2 bipartite system density matrix expanded with $|\uparrow\uparrow\rangle, |\uparrow\downarrow\rangle, |\downarrow\uparrow\rangle, |\downarrow\downarrow\rangle$ is given by

$$\rho = \frac{1}{4} \left(\mathbf{I}_4 + \sum_i B_i^+ \sigma^i \otimes \mathbf{I}_2 + \sum_j B_j^- \mathbf{I}_2 \otimes \sigma^j + \sum_{i,j} C_{ij} \sigma^i \otimes \sigma^j \right), \quad (1)$$

where \mathbf{I}_n is an $n \times n$ unit matrix, and $\sigma^{i,j}$ are the Pauli matrices representing the spin directions. We use bold-face symbols to represent square matrices. The size of QE can be quantified by concurrence [11]

$$\mathcal{C}(\rho) = \max(0, 2\lambda_{\max} - \text{Tr}(\mathcal{R})), \quad (2)$$

where $\mathcal{R} = \sqrt{\sqrt{\rho}(\sigma_y \otimes \sigma_y)\rho^*(\sigma_y \otimes \sigma_y)\sqrt{\rho}}$, and λ_{\max} is its largest eigenvalue. It satisfies $0 \leq \mathcal{C} \leq 1$ with $\mathcal{C} = 0$ indicating a vanishing and $\mathcal{C} = 1$ a maximal entanglement, respectively. A relatively stronger requirement of entanglement than the concurrence is the violation of the

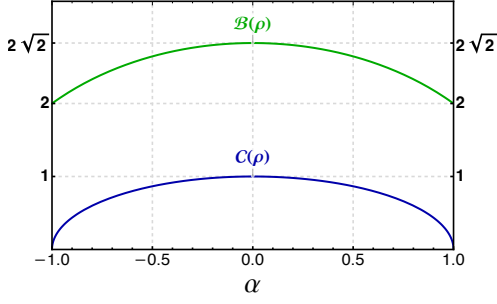


Fig. 1. Concurrence $\mathcal{C}(\rho)$ and the CHSH parameter $\mathcal{B}(\rho)$ in the spin-0 case.

BI. An example of this is the Clauser-Horne-Shimony-Holt (CHSH) parameter $\mathcal{B}(\rho)$ which is bounded by 2 in any classical theories. However, in a quantum one, its maximum is $2\sqrt{2}$ and given by [12, 13]

$$\mathcal{B}(\rho) = 2\sqrt{\mu_1^2 + \mu_2^2} \leq 2\sqrt{2}, \quad (3)$$

where μ_i^2 are the eigenvalues of the $\mathbf{C}^T \mathbf{C}$ in the order of $\mu_1^2 \geq \mu_2^2 \geq \mu_3^2$ with $(\mathbf{C})_{ij} = C_{ij}$ and $\mathcal{B}(\rho) > 2$ signals the Bell nonlocality.

Formalism.—We set up the formalism for $i \rightarrow f_1 \bar{f}_2$ with i either a spin-0 or a spin-1 particle in this section. For a spin-0 particle h_i , the amplitude is generically parameterized as

$$M_{\text{scalar}} = \bar{f}_1 (g_S - g_P \gamma_5) f_2, \quad (4)$$

with $g_{S(P)}$ the (pseudo)-scalar coupling. If g_S and g_P are both nonzero, P is violated. The spinless mother particle would lead to a pure final state given by:

$$|\Psi\rangle = \frac{S+P}{\sqrt{2(|S|^2 + |P|^2)}} |\uparrow\downarrow\rangle + \frac{S-P}{\sqrt{2(|S|^2 + |P|^2)}} |\downarrow\uparrow\rangle, \quad (5)$$

where the arrows represent the spins of f_1 and \bar{f}_2 in order along the momentum direction of f_1 denoted as \hat{k} throughout this work. Here, $S = \sqrt{m_i^2 - (m_1 + m_2)^2} g_S$,

$P = \sqrt{m_i^2 - (m_1 - m_2)^2} g_P$, and m_i and $m_{1,2}$ are the masses of h_i and $f_{1,2}$, respectively. It is then straightforward to obtain from eq. (5) that

$$\vec{B}^\pm = \pm \alpha \hat{k}, \quad C_{ij} = \gamma \delta_{ij} - (1 + \gamma) \hat{k}_i \hat{k}_j + \beta \epsilon^{ijk} \hat{k}_k, \quad (6)$$

with the Lee-Yang parameters [14]

$$\alpha = \frac{2\text{Re}(S^* P)}{|S|^2 + |P|^2}, \quad \beta = \frac{2\text{Im}(S^* P)}{|S|^2 + |P|^2}, \quad \gamma = \frac{|S|^2 - |P|^2}{|S|^2 + |P|^2}. \quad (7)$$

From their definitions, the concurrence and the CHSH parameters in this scenario are given by

$$\mathcal{C}(\rho) = \sqrt{1 - \alpha^2}, \quad \mathcal{B}(\rho) = 2\sqrt{2 - \alpha^2}, \quad (8)$$

which we also depict in Fig. 1 in blue and green, respectively. As is clearly seen, the daughter particles disentangle completely with $\mathcal{C}(\rho) = 0$ for the maximal value $|\alpha| = 1$, or equivalently $S = \pm P$. At this value $\mathcal{B}(\rho) = 2$ is the boundary of classical and quantum theories and therefore cannot distinguish these two theories. The physical reason for this can be understood from $|\Psi\rangle$ in eq. (5), where only one of the two terms survives, leading to a disentangled bipartite state and suggesting a preference for particular spin combinations and a decrease in QE from P violation. Apart from this special limit, both $\mathcal{C}(\rho)$ and $\mathcal{B}(\rho)$ increase with decreasing $|\alpha|$ and saturate at their respective upper bounds in the optimal limit where $\alpha \rightarrow 0$.

For a spin-1 vector V , we consider its on-shell production at a lepton collider and its subsequent decay into a spin-1/2 fermion pair denoted as $e^+ e^- \rightarrow V \rightarrow f \bar{f}$. To address the P-violating effects on QE and BI, we parameterize the decay amplitude as

$$M_{\text{vector}} = \epsilon_\mu \bar{u} \gamma^\mu (F_V + F_A \gamma_5) v, \quad (9)$$

where ϵ_μ is the polarization vector of V , u and v are the Dirac spinors, $F_{V(A)}$ is the (axial-)vector coupling, and we leave out any possible dipole interactions that can also exist in the most general case. Denoting 3-momenta of e^- and f as \hat{p} and \hat{k} , \vec{B}^\pm and C_{ij} are [15]

$$\begin{aligned} \vec{B}^\pm &= \frac{1}{\bar{N}} \sqrt{1 - y_m^2} \left(y_m c_\theta \hat{p} + (1 + (1 - y_m) c_\theta^2) \hat{k} \right) \text{Re} \left(\frac{F_A}{F_V} \right), \\ C_{ij} &= \frac{1}{\bar{N}} \left[\frac{1}{3} \bar{N} \delta_{ij} + (1 - (1 - y_m^2) \left| \frac{F_A}{F_V} \right|^2) (\hat{p}_i \hat{p}_j - \frac{1}{3} \delta_{ij}) - ((1 - y_m) c_\theta (1 - (1 + y_m) \left| \frac{F_A}{F_V} \right|^2)) (\hat{p}_i \hat{k}_j + \hat{k}_i \hat{p}_j - \frac{2}{3} c_\theta \delta_{ij}) \right. \\ &\quad \left. + (1 - y_m) (1 + c_\theta^2 (1 - y_m)) (\hat{k}_i \hat{k}_j - \frac{1}{3} \delta_{ij}) + \sqrt{1 - y_m^2} s_\theta \left((\hat{p}_i \hat{n}_j + \hat{n}_i \hat{p}_j) - (1 - y_m) c_\theta (\hat{k}_i \hat{n}_j + \hat{n}_i \hat{k}_j) \right) \text{Im} \left(\frac{F_A}{F_V} \right) \right], \\ \bar{N} &= \frac{1}{2} \left[1 + c_\theta^2 + y_m^2 s_\theta^2 + (1 - y_m^2) (1 + c_\theta^2) \left| \frac{F_A}{F_V} \right|^2 \right], \end{aligned} \quad (10)$$

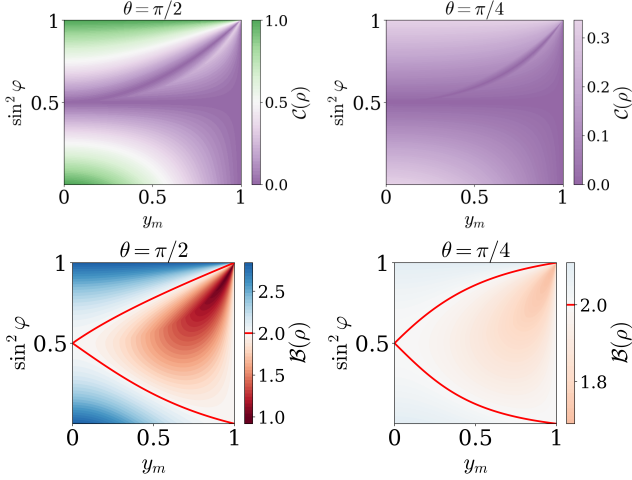


Fig. 2. Dependencies of $\mathcal{C}(\rho)$ (upper panels) and $\mathcal{B}(\rho)$ (lower panels) on y_m and s_φ^2 at $\theta = \pi/2$ (left panels) and $\theta = \pi/4$ (right panels). The blue regions outside the red line represent the parameter spaces where $\mathcal{B}(\rho) > 2$, prohibited in a local hidden-variable theory.

where $y_m = 2m_f/m_V$ with m_V and m_f masses of the mother and the daughter particles, $\hat{n} = \hat{p} \times \hat{k}/s_\theta$ with $c_\theta \equiv \cos \theta = \hat{p} \cdot \hat{k}$ and $s_\theta \equiv \sin \theta$. Here we have neglected P violation in $e^+e^- \rightarrow V$. The full expression with it is given in the end matter of this letter and will be fully taken into account numerically in the next section.

Interestingly, we note that $C_{ij} \rightarrow \hat{p}_i \hat{p}_j = \hat{k}_i \hat{k}_j$ with $\theta \rightarrow 0$ or π such that C_{ij} becomes respecting the parity symmetry. Furthermore, $\mathcal{C}(\rho) \rightarrow 0$ and $\mathcal{B}(\rho) \rightarrow 2$ in this far forward or backward region and the daughter pair tends to disentangle entirely and the BI also becomes fulfilled. Experimentally, the forward and the backward regions are largely avoided practically for the spin reconstruction of daughter particles due to very large background, we therefore focus our discussion on the phase space away from $\theta \rightarrow 0$ and π in the following.

For simplicity but without sacrificing any physical importance for the discussion below, we assume F_A/F_V to be real from here on and define $\tan \varphi = F_A/F_V$ along with $(c_\varphi, s_\varphi) = (\cos \varphi, \sin \varphi)$. The concurrence and the CHSH parameters then become more complicated due to extra freedoms compared with the spin-0 case above. We thus opt to present their numerical results in Fig. 2, where the lower row is for $\mathcal{B}(\rho)$ with $\mathcal{B}(\rho) \leq 2$ as embraced by the two red curves to the right, and the upper row for $\mathcal{C}(\rho)$. Furthermore, similar to $\theta \rightarrow 0$ or π as discussed in the previous paragraph, we observe from Fig. 2 that the daughter pair also disentangles completely when $y_m \rightarrow 1$ since $C_{ij} \rightarrow \hat{p}_i \hat{p}_j$ under this limit. From the above discussions we see that just like the spin-0 cases the level of QE and the size of BI violation are intricately dictated by the interaction forms. In turn, the fundamental interactions can be inferred from the patterns in QE and BI

violations.

On the transverse production plane at $\theta = \pi/2$ with $y_m = 0$, we obtain

$$\mathcal{C}(\rho)_{\theta=\pi/2} = \sqrt{1 - \alpha_f^2}, \quad \mathcal{B}(\rho)_{\theta=\pi/2} = 2\sqrt{2 - \alpha_f^2}. \quad (11)$$

Here, $\alpha_f = 2s_\varphi c_\varphi$ represents the polarization of $V \rightarrow f\bar{f}$ and quantifies the size of the P violation. One immediately recognizes its similarity to the spin-0 case in eq. (5). Note that the maximal values of $\mathcal{B}(\rho)$ and $\mathcal{C}(\rho)$ are always achieved on the transverse production plane at $\theta = \pi/2$. With $y_m = 0$, the final state becomes a pure one:

$$|\Psi\rangle_{\theta=\pi/2} = \frac{1}{\sqrt{2}} [(c_\varphi + s_\varphi) |\uparrow\uparrow\rangle + (c_\varphi - s_\varphi) |\downarrow\downarrow\rangle]. \quad (12)$$

For $\tan \varphi = \pm 1$, the final state is disentangled, $\mathcal{B}(\rho)$ and $\mathcal{C}(\rho)$ reach their minima and fall on the boundaries of classical or local hidden-variable theories.

In addition, the analogy between eq. (5) and eq. (12) also renders our discussion on parity in the spin-0 case applicable to this spin-1 scenario but in a different context: both $\mathcal{C}(\rho)$ and $\mathcal{B}(\rho)$ will also saturate their upper bounds with $s_\varphi^2 \rightarrow 0$ and 1 as seen from the upper- and the lower-left corners in the left column of Fig. 2. A similar conclusion can be drawn away from the transverse production plane as showcased in the right column of Fig. 2 with $\theta = \pi/4$. Therefore, it is possible to enhance the effects from parity on entanglement and Bell nonlocality by covering a larger phase space around $\theta = \pi/2$. The average in phase space will in turn change the quantum nature of the bipartite system and thus the tests of BI. We discuss this issue from measurements in the next section.

Measurements of QE and BI.—The phase space average mentioned in the last section is effectively taken over a set of quantum states represented by ρ_a , and the resulting state is a fictitious one [6] which we denote as $\bar{\rho} = \sum_a^N \rho_a/N$ with N the total number of states. Since ρ_a is obviously frame-dependent, the optimal choice of the frame is therefore the one to maximize the CHSH parameter of the fictitious state

$$\bar{\mathcal{B}}(\rho) = \max(\mathcal{B}(\bar{\rho}')) = \frac{2}{N} \sqrt{\sum_{i=1,2} \left(\sum_a^N \mu_i^a \right)^2}, \quad (13)$$

from an $SU(2) \otimes SU(2)$ rotation U_a such that $\bar{\rho}' = \sum_a^N U_a \rho_a U_a^T / N$. $\mu_{1,2}^a$ here are the largest two eigenvalues of \mathbf{C}_a and can always be taken as positive from an $SU(2) \otimes SU(2)$ rotation. The proof of Eq. (13) can be found in Ref. [16], and we provide an alternative in the end matter.

Now we discuss the most general form of ρ based on fundamental symmetries without the restrictions of the QFT for spin-0 and spin-1 systems. For a spin-0 h_i and

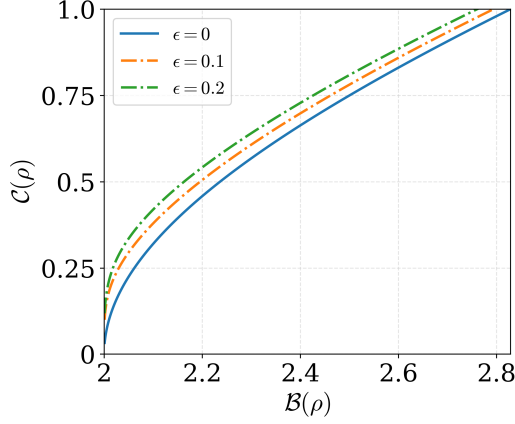


Fig. 3. Relationship between $\mathcal{C}(\rho)$ and $\mathcal{B}(\rho)$. The one-to-one correspondence between $\mathcal{C}(\rho)$ and $\mathcal{B}(\rho)$ is disrupted by nonzero ϵ for illustrations. The blue line represents the predictions from the QFT, where a nonzero ϵ cannot be generated under standard QFT assumptions.

its decay $h_i \rightarrow f_1 \bar{f}_2$, there is only one freedom in the rest frame of h_i being the momentum of f_1 . Therefore, the most general forms for \vec{B}^\pm and \mathbf{C} are

$$\begin{aligned} \vec{B}^+ &= b_{1k} \hat{k}, \quad \vec{B}^- = b_{2k} \hat{k}, \\ C_{ij} &= c_0 \delta_{ij} + c_2 \epsilon_{ijl} \hat{k}_l + c_5 (\hat{k}_i \hat{k}_j - \delta_{ij}/3). \end{aligned} \quad (14)$$

Due to the absence of any orbital angular momentum along the direction of \hat{k} , the spins of the final states must be opposite, $\rho(\vec{s}_1 = \vec{s}_2 = \pm \hat{k}) = 0$, where \vec{s}_1 and \vec{s}_2 are the spins of f_1 and \bar{f}_2 , respectively. This immediately leads to $b_{1k} = -b_{2k}$, and $c_0 = -1 - 2c_5/3$, and the spin-0 system is completely described by three parameters. From eq. (14), we have that $\mathcal{B}(\rho) = 2\sqrt{2} - b_{1k}^2 - \epsilon$ and

$$\mathcal{C}(\rho) = \frac{1}{2} [(\mathcal{B}(\rho)^2 - 4)(\mathcal{B}(\rho)^2 - 4 + 4\epsilon)]^{\frac{1}{4}}, \quad (15)$$

where $\epsilon = 1 - b_{1k}^2 - c_2^2 - (1 + c_5)^2 \geq 0$ to guarantee non-negative probability. The relationship between $\mathcal{C}(\rho)$ and $\mathcal{B}(\rho)$ are depicted in Fig. 3, where the one-to-one correspondence between $\mathcal{C}(\rho)$ and $\mathcal{B}(\rho)$ is broken by a nonzero ϵ . In the QFT limit, we have that $c_5 = -1 - \gamma$, $c_2 = \beta$ and $b_{1k} = \alpha$ and $\epsilon = 0$ is guaranteed. Therefore, nonzero ϵ provides a novel method to test the effects beyond the QFT. We emphasize that these parameters can be determined by measuring the cascade decays of f_1 and \bar{f}_2 , described by the end matter of this work. We point out that this examination of $\epsilon \neq 0$ can also be performed using hyperon decays [17].

In this case, we propose testing of the BI with the unexplored weak decay channels $B \rightarrow \mathbf{B}_c \bar{\mathbf{B}}'_c$, which is well-suited for LHCb and Belle II [18–20]. Here, $B = (B^+, B^0, B_s^0)$ and $\mathbf{B}_c^{(\prime)} = (\Lambda_c^+, \Xi_c^+, \Xi_c^0)$. For all these channels, $\alpha \neq 0$ due to parity violation and the violation of BI is expected. We also point it out that it will be

interesting to consider neutral B_s mesons that are CP-tagged as B_{sL}^0/B_{sH}^0 . For these neutral mesons, by ignoring the tiny CP violation from the mixing, $B_{sL}^0/B_{sH}^0 \rightarrow \mathbf{B}_c \bar{\mathbf{B}}_c$ conserve CP, leading to $b_{1k} = c_2 = 0$ in both cases, with c_5 being -2 and 0 , respectively, for B_{sL}^0 and B_{sH}^0 . As a consequence, they are ideal candidates for a maximal violation of the BI. Similar analysis can be carried out in the $h \rightarrow f\bar{f}$ at the LHC or future colliders.

On the other hand, for the spin-1 case, \vec{B}^\pm and \mathbf{C} contain three and nine matrix elements, expanded by \hat{l} with $\hat{l} = \hat{p}, \hat{k}, \hat{n}$. CP symmetry constrains \mathbf{C} to be symmetric and $\vec{B}^+ = \vec{B}^-$, and one then has nine free parameters in total. In this scenario, we promote $e^+e^- \rightarrow Z \rightarrow f\bar{f}$ with Z produced on-shell and consider the decay in the Standard Model with $f = b, c, \tau$ [21]. The Lagrangian is parameterized as

$$\mathcal{L}_{Zff} = -\frac{g_L}{2 \cos \theta_W} Z_\mu \bar{f} \gamma^\mu (g_V - g_A \gamma_5) f, \quad (16)$$

where g_L is the weak coupling constant, $g_V = I_f^3 - 2Q_f \sin^2 \theta_W$ and $g_A = I_f^3$ with I_f^3 and Q_f the isospin and electric charge of f . Here, θ_W is the Weinberg angle of the weak interaction. According to the heavy quark symmetry, spins of $\Lambda_{b,c}$ contribute exclusively from the heavy quarks b and c . Hence, to the leading order, the Lagrangian for $\Lambda_{b,c}$ can be obtained by replacing f by Λ_f in eq. (16) [22], together with an overall hadronization factor g_Λ whose explicit number does not enter the discussion for testing QE and the violation of the BI.

Processes	$-\alpha_f$	$\bar{\mathcal{B}}_{-1.0}^{-0.5}$	$\bar{\mathcal{B}}_{-0.5}^{-0.3}$	$\bar{\mathcal{B}}_{-0.3}^{-0.1}$	$\bar{\mathcal{B}}_{-0.1}^{0.1}$	$\bar{\mathcal{B}}_{0.1}^{0.3}$	$\bar{\mathcal{B}}_{0.3}^{0.5}$	$\bar{\mathcal{B}}_{0.5}^{1.0}$
$Z \rightarrow \Lambda_b^0 \bar{\Lambda}_b^0$	0.94	2.01	2.04	2.08	2.10	2.10	2.06	2.01
$Z \rightarrow \Lambda_c^+ \bar{\Lambda}_c^-$	0.70	2.03	2.24	2.40	2.49	2.46	2.31	2.05
$Z \rightarrow \tau^- \tau^+$	0.21	2.06	2.45	2.69	2.81	2.71	2.47	2.07

Table I. The numerical values of $\bar{\mathcal{B}}_{\omega_2}^{\omega_1}$ in $Z \rightarrow f\bar{f}$, where $\bar{\mathcal{B}}_{\omega_2}^{\omega_1}$ is the average of $\bar{\mathcal{B}}$ over the range $\omega_2 > c_\theta > \omega_1$. $\alpha_{\Lambda_{b,c}}$ are calculated in the heavy quark limit.

For spin-1 cases, measurements of \mathcal{B} requires averaging over θ according to Eq. (13). We define

$$\bar{\mathcal{B}}_{\omega_1}^{\omega_2} = \frac{2}{\mathcal{R}_{\omega_1}^{\omega_2}} \sqrt{\sum_{i=1,2} \left[\int_{\omega_1}^{\omega_2} \mu_i(c_\theta) \left(\frac{d\sigma}{dc_\theta} \right) dc_\theta \right]^2}, \quad (17)$$

where $\mathcal{R}_{\omega_1}^{\omega_2} = \int_{\omega_1}^{\omega_2} (d\sigma/dc_\theta) dc_\theta$ and σ is the scattering rate. Note that $\bar{\mathcal{B}}_{\omega_1}^{\omega_2} = \bar{\mathcal{B}}_{-\omega_2}^{-\omega_1}$ up to $\mathcal{O}(d_J)$, where d_J is the P-violating parameter on the production side, as detailed in the end matter. The numerical values of $\bar{\mathcal{B}}$ are documented in Table I. From the table, one observes that a larger α_f^2 leads to lower QE, and $\mathcal{B}(\rho)$ reaches its largest values around $\theta = \pi/2$, as anticipated. An interesting feature is that the BI is violated in every bin. Genuine P-violating effects are found to be negligible in

J/ψ baryonic decays, and $\bar{\mathcal{B}}_{\omega_1}^{\omega_2} = \bar{\mathcal{B}}_{-\omega_2}^{\omega_1}$ holds up to 10^{-4} , while the magnetic field affects $\bar{\mathcal{B}}$ at $\mathcal{O}(10^{-3})$ as detailed in the next section.

External magnetic field effects.—We now study the effects of the interaction between the environmental external magnetic field and the system on QE and BI. In actual situation, the external magnetic field \vec{H} inside the detector is utilized to reconstruct the momenta of charged particles as well as a measure of their spin orientation. We argue in the following that the existence of a nonzero \vec{H} can introduce a deviation to the density matrix ρ . Such effects have been ignored in literature.

We take the external magnetic field \vec{H} near the production point, which coincides with the beam axis, as \hat{z} with a magnitude of 1 tesla [23–27], and the production plane of the charged daughter pair as $\hat{x} - \hat{z}$. \vec{H} rotates the momentum by

$$\hat{l}(t) = \exp\left(-i\vec{J} \cdot \frac{2q\vec{H}}{m_V}t\right)\hat{l}(0), \quad (18)$$

with $(\vec{J}_i)_{jk} = -i\varepsilon_{ijk}$ the SO(3) generators and q the electric charge.

For the cases of Ξ^- , Λ_c^+ and τ^- interested to us, since their Larmor frequencies multiplied by their individual lifetimes are found to be about 1.3%, 1.0×10^{-4} and 8.7×10^{-4} , respectively, it then suffices to truncate at the first Magnus expansion for the spin precession. We obtain

$$\vec{s}_1(t_1) = e^{-i\Omega_1(t_1)}\vec{s}_1(0), \quad \vec{s}_2(t_2) = e^{i\Omega_1(t_2)}\vec{s}_2(0). \quad (19)$$

with

$$\Omega_1 = \int_0^t dt' \vec{J} \cdot \frac{gq}{2m_f y_m} \left[\vec{H} + (y_m - 1)\vec{H} \cdot \hat{k}\hat{k}(t') \right], \quad (20)$$

where g is the gyromagnetic ratio, and note that \vec{s}_1 and \vec{s}_2 rotate oppositely due to their opposite magnetic dipole moments.

The modified ρ is then obtained upon replacing momenta and spins at the production time by those at the decay time, and its time average is calculated with a Gaussian distribution $p(t_1, t_2)$ given by

$$p(t_1, t_2) = \frac{1}{2\pi\sigma_{\text{TOF}}^2} e^{-\frac{(t_1 - \tau)^2 + (t_2 - \tau)^2}{2\sigma_{\text{TOF}}^2}}, \quad (21)$$

with σ_{TOF} the time resolution of the time-of-flight (TOF) system of the detector which is 65/2 ps for BESIII [28] and 300/2 ps as the typical value for LEP detectors [24–27], such that

$$\bar{\rho} = \int dt_1 dt_2 \rho(t_1, t_2) p(t_1, t_2), \quad \bar{C}_{ij} = \text{Tr}[\bar{\rho}\sigma_i \otimes \sigma_j]. \quad (22)$$

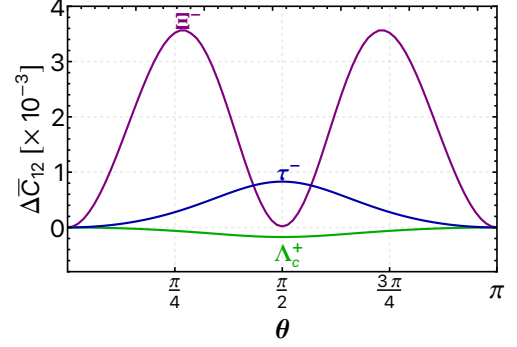


Fig. 4. Spurious P and/or CP violating effects from the external magnetic field for $J/\psi \rightarrow \Xi^- \Xi^+$ (purple), and $Z \rightarrow \Lambda_c^+ \bar{\Lambda}_c^-$ (green) and $\tau^- \tau^+$ (blue), where θ is the production angle of the final state particle.

Numerically, we find the influence on \mathcal{B} from the external \vec{H} field marginal. Modifications to the spin correlation matrix C_{ij} are found important. We illustrate this point in Fig. 4, where the y -axis is defined as

$$\Delta\bar{C}_{12} \equiv \bar{C}_{12} - \bar{C}_{21}. \quad (23)$$

Since $C_{12} = C_{21}$ in the P- and CP-conserving limit, $\Delta\bar{C}_{12}$ gives a net measure on the magnetic effect. As is clearly seen from the plot, the presence of a non-vanishing magnetic field can induce spurious P and/or CP violating effects, which in turn produces a nonzero $\Delta\bar{C}_{12}$ of $\mathcal{O}(10^{-3})$ for $J/\psi \rightarrow \Xi^- \Xi^+$, and of $\mathcal{O}(10^{-4})$ for $Z \rightarrow \Lambda_c^+ \bar{\Lambda}_c^-$, $\tau^- \tau^+$ as shown in Fig. 4. On the other hand, since C_{ij} is directly related to the differential angular distribution as shown in the end matter, such a spurious effect has to be isolated from the fitting to obtain a genuine determination of P and/or CP violation. Moreover, if this effect is not subtracted in the analysis and the bipartite system is assumed to be isolated as before, one may falsely draw the conclusion of invalidity of the QFT as similarly depicted in Fig. 3.

The nonzero $\Delta\bar{C}_{ij}$ are detectable through the cascade decays of the daughter fermions, $f \rightarrow f'X$ and $\bar{f} \rightarrow \bar{f}'X$ with f' a fermion and X the rest of the particles. Ideal choices of the cascade decays, for instance, are $\Xi^- \rightarrow \Lambda\pi^-$, $\Lambda_b^0 \rightarrow \Lambda_c^+\pi^-$, $\Lambda_c^+ \rightarrow \Lambda\pi^-$, and $\tau^- \rightarrow \pi^-\nu_\tau$ [29], as described in the end matter. Measurements would be able to carry out at next-generation colliders such as STCF [30, 31], CEPC [32] and FCC-ee [33].

Acknowledgements—This work was partially supported by the Fundamental Research Funds for the Central Universities, by NSFC grant numbers 11821505, 11935017, 12075299, 12090064, 12205063, 12347116 and 12375088, by the Strategic Priority Research Program of Chinese Academy of Sciences grant number XDB34000000, by CPSF grant numbers 2023M732255, 2023M742293 and GZC20231613.

* yongdu5@sjtu.edu.cn

† hexg@sjtu.edu.cn

‡ chiaweiliu@sjtu.edu.cn

§ majp@itp.ac.cn

- [1] A. Einstein, B. Podolsky, and N. Rosen, “Can quantum mechanical description of physical reality be considered complete?,” *Phys. Rev.* **47** (1935) 777–780.
- [2] J. S. Bell, “On the Einstein-Podolsky-Rosen paradox,” *Physics Physique Fizika* **1** (1964) 195–200.
- [3] V. D. Barger, J. Ohnemus, and R. J. N. Phillips, “Spin Correlation Effects in the Hadroproduction and Decay of Very Heavy Top Quark Pairs,” *Int. J. Mod. Phys. A* **4** (1989) 617.
- [4] **ATLAS**, G. Aad *et al.*, “Observation of quantum entanglement in top-quark pairs using the ATLAS detector,” [arXiv:2311.07288](#).
- [5] **CMS**, “Observation of quantum entanglement in top quark pair production in proton-proton collisions at $\sqrt{s} = 13$ TeV,” [arXiv:2406.03976](#).
- [6] Y. Afik and J. R. M. n. de Nova, “Entanglement and quantum tomography with top quarks at the LHC,” *Eur. Phys. J. Plus* **136** (2021) no. 9, 907, [arXiv:2003.02280](#).
- [7] S. Wu, C. Qian, Q. Wang, and X.-R. Zhou, “Bell nonlocality and entanglement in $e^+e^- \rightarrow Y\bar{Y}$ at *BESIII*,” [arXiv:2406.16298](#).
- [8] J. Bernabeu, F. Martinez-Vidal, and P. Villanueva-Perez, “Time Reversal Violation from the entangled B^0 -anti B^0 system,” *JHEP* **08** (2012) 064, [arXiv:1203.0171](#).
- [9] **BaBar**, J. P. Lees *et al.*, “Observation of Time Reversal Violation in the B^0 Meson System,” *Phys. Rev. Lett.* **109** (2012) 211801, [arXiv:1207.5832](#).
- [10] **BESIII**, M. Ablikim *et al.*, “Probing CP symmetry and weak phases with entangled double-strange baryons,” *Nature* **606** (2022) no. 7912, 64–69, [arXiv:2105.11155](#).
- [11] W. K. Wootters, “Entanglement of formation of an arbitrary state of two qubits,” *Phys. Rev. Lett.* **80** (1998) 2245–2248, [arXiv:quant-ph/9709029](#).
- [12] J. F. Clauser, M. A. Horne, A. Shimony, and R. A. Holt, “Proposed experiment to test local hidden variable theories,” *Phys. Rev. Lett.* **23** (1969) 880–884.
- [13] J. F. Clauser and M. A. Horne, “Experimental Consequences of Objective Local Theories,” *Phys. Rev. D* **10** (1974) 526.
- [14] T. D. Lee and C.-N. Yang, “General Partial Wave Analysis of the Decay of a Hyperon of Spin 1/2,” *Phys. Rev.* **108** (1957) 1645–1647.
- [15] Y. Du, X.-G. He, J.-P. Ma, and X.-Y. Du, “Fundamental Tests of P and CP Symmetries Using Octet Baryons at the J/ψ Threshold,” [arXiv:2405.09625](#).
- [16] K. Cheng, T. Han, and M. Low, “Optimizing Entanglement and Bell Inequality Violation in Top Anti-Top Events,” [arXiv:2407.01672](#).
- [17] **Particle Data Group**, R. L. Workman *et al.*, “Review of Particle Physics,” *PTEP* **2022** (2022) 083C01.
- [18] **LHCb**, R. Aaij *et al.*, “Study of beauty hadron decays into pairs of charm hadrons,” *Phys. Rev. Lett.* **112** (2014) 202001, [arXiv:1403.3606](#).
- [19] **Belle**, Y. B. Li *et al.*, “First Measurements of Absolute Branching Fractions of the Ξ_c^0 Baryon at Belle,” *Phys. Rev. Lett.* **122** (2019) no. 8, 082001, [arXiv:1811.09738](#).
- [20] **Belle**, Y. B. Li *et al.*, “First measurements of absolute branching fractions of the Ξ_c^+ baryon at Belle,” *Phys. Rev. D* **100** (2019) no. 3, 031101, [arXiv:1904.12093](#).
- [21] H. K. Dreiner, “Bell’s inequality and tau physics at LEP,” in *2nd Workshop on Tau Lepton Physics*. 10, 1992. [arXiv:hep-ph/9211203](#).
- [22] B. Mele and G. Altarelli, “Lepton spectra as a measure of b quark polarization at LEP,” *Phys. Lett. B* **299** (1993) 345–350.
- [23] **BESIII**, M. Ablikim *et al.*, “Design and Construction of the *BESIII* Detector,” *Nucl. Instrum. Meth. A* **614** (2010) 345–399, [arXiv:0911.4960](#).
- [24] **L3**, B. Adeva *et al.*, “The Construction of the *L3* Experiment,” *Nucl. Instrum. Meth. A* **289** (1990) 35–102.
- [25] **ALEPH**, D. Decamp *et al.*, “ALEPH: A detector for electron-positron annihilations at LEP,” *Nucl. Instrum. Meth. A* **294** (1990) 121–178. [Erratum: *Nucl. Instrum. Meth. A* 303, 393 (1991)].
- [26] **OPAL**, K. Ahmet *et al.*, “The OPAL detector at LEP,” *Nucl. Instrum. Meth. A* **305** (1991) 275–319.
- [27] **DELPHI**, P. A. Aarnio *et al.*, “The DELPHI detector at LEP,” *Nucl. Instrum. Meth. A* **303** (1991) 233–276.
- [28] Y.-X. Guo *et al.*, “The study of time calibration for upgraded end cap TOF of *BESIII*,” *Radiat. Detect. Technol. Methods* **1** (2017) 15.
- [29] **LHCb**, R. Aaij *et al.*, “Measurement of Λ_b^0 , Λ_c^+ and Λ decay parameters using $\Lambda_b^0 \rightarrow \Lambda_c^+ h^-$ decays,” [arXiv:2409.02759](#).
- [30] **Charm-Tau Factory**, A. E. Bondar *et al.*, “Project of a Super Charm-Tau factory at the Budker Institute of Nuclear Physics in Novosibirsk,” *Phys. Atom. Nucl.* **76** (2013) 1072–1085.
- [31] M. Achasov *et al.*, “STCF conceptual design report (Volume 1): Physics & detector,” *Front. Phys. (Beijing)* **19** (2024) no. 1, 14701, [arXiv:2303.15790](#).
- [32] **CEPC Study Group**, M. Dong *et al.*, “CEPC Conceptual Design Report: Volume 2 - Physics & Detector,” [arXiv:1811.10545](#).
- [33] **FCC**, A. Abada *et al.*, “FCC-ee: The Lepton Collider: Future Circular Collider Conceptual Design Report Volume 2,” *Eur. Phys. J. ST* **228** (2019) no. 2, 261–623.

End matter for “Impact of parity violation on quantum entanglement and Bell nonlocality”

MAXIMUM OF $\mathcal{B}(\bar{\rho})$ FOR A FICTITIOUS STATE

Lemma: There exist matrices \mathbf{R}_\pm such that $\mathbf{R}_+ \mathbf{C} \mathbf{R}_- = \text{diag}(\mu_1, \mu_2, \dots, \mu_N)$ with \mathbf{C} an arbitrary $N \times N$ real matrix and $\mathbf{R}_\pm \in SO(N)$. Furthermore, $\mu_i \geq |\mu_{i+1}|$ for $i = \{1, 2, \dots, N-1\}$.

Since $\mathbf{C}^T \mathbf{C}$ is semipositive and symmetric, there exists a matrix $\mathbf{R} \in SO(N)$ such that $\mathbf{R}^T \mathbf{C}^T \mathbf{C} \mathbf{R} = \text{diag}(\mu_1^2, \mu_2^2, \dots, \mu_N^2)$ with the hierarchical order $\mu_1^2 \geq \mu_2^2 \geq \dots \geq \mu_N^2$. Given that $(\mathbf{R} \mathbf{C} \mathbf{R})^T (\mathbf{R} \mathbf{C} \mathbf{R})$ is diagonal, we must have

$$\mathbf{R} \mathbf{C} \mathbf{R} = \begin{pmatrix} \mu_1 \hat{v}_1^T, & \mu_2 \hat{v}_2^T, & \dots, & \mu_N \hat{v}_N^T \end{pmatrix}, \quad (24)$$

where μ_i are real constants, $\hat{v}_i = ((\hat{v}_i)_1, (\hat{v}_i)_2, \dots, (\hat{v}_i)_N)$ and $\hat{v}_i \cdot \hat{v}_j = \delta_{ij}$. Define

$$\mathbf{R}'^T = \begin{pmatrix} \text{sgn}(\mu_1) \hat{v}_1, & \text{sgn}(\mu_2) \hat{v}_2, & \dots, & \left(\prod_{i=1}^{N-1} \text{sgn}(\mu_i) \right) \hat{v}_N \end{pmatrix} \in SO(N). \quad (25)$$

With $\hat{v}_i \cdot \hat{v}_j = \delta_{ij}$, we see that $\mathbf{R}' (\mathbf{R} \mathbf{C} \mathbf{R}) = \text{diag}(|\mu_1|, |\mu_2|, \dots, \left(\prod_{i=1}^{N-1} \text{sgn}(\mu_i) \right) \mu_N)$. By identifying $\mathbf{R}' \mathbf{R} = \mathbf{R}_+$ and $\mathbf{R} = \mathbf{R}_-$, we prove the lemma. The proof also provides a concrete method to obtain \mathbf{R}_\pm from \mathbf{C} . ■

The spin-correlation matrix of a fictitious density matrix is given by

$$\bar{\mathbf{C}} = \frac{1}{N} \sum_a \mathbf{C}_a = \frac{1}{N} \sum_a \mathbf{R}_+^a \mathbf{C}_{\text{diag}}^a \mathbf{R}_-^a, \quad (26)$$

where $\mathbf{C}_{\text{diag}}^a = \text{diag}(\mu_1^a, \mu_2^a, \mu_3^a)$. We have used the above lemma to diagonalize \mathbf{C}_a and chosen $\mu_1^a \geq \mu_2^a \geq |\mu_3^a|$. Likewise, we diagonalize $\bar{\mathbf{C}} = \text{diag}(\mu_1, \mu_2, \mu_3)$ with $\mu_1 \geq \mu_2 \geq |\mu_3|$. It is important to note that $\mu_{1,2,3}$ depend on the chosen basis or equivalently the choice of \mathbf{R}_\pm^a . In the following $\mu_{1,2,3}$ are named as $\bar{\mu}_{1,2,3}$ when $\mathbf{R}_\pm^a = \mathbf{I}_3$ for all a . Eq. (13) is equivalent to the statement of that $\bar{\mu}_1^2 + \bar{\mu}_2^2 \geq \mu_1^2 + \mu_2^2$, of which we aim to prove now.

Since $\mu_1^a \geq \mu_2^a \geq |\mu_3^a|$, we have that

$$(\mathbf{R}_+^a \mathbf{C}_{\text{diag}}^a \mathbf{R}_-^a)_{11} \leq \mu_1^a (\mathbf{R}_+^a \mathbf{R}_-^a)_{11}. \quad (27)$$

Summing the index of a and note $1 \geq (\mathbf{R}_+^a \mathbf{R}_-^a)_{11}$, we arrive at $\mu_1 \leq \bar{\mu}_1$. For $\mu_1 + \mu_2$, we find

$$\begin{aligned} & (\mathbf{R}_+^a \mathbf{C}_{\text{diag}}^a \mathbf{R}_-^a)_{11} + (\mathbf{R}_+^a \mathbf{C}_{\text{diag}}^a \mathbf{R}_-^a)_{22} \leq (\mu_1^a - \mu_2^a) ((\mathbf{R}_+^a)_{11} (\mathbf{R}_-^a)_{11} + (\mathbf{R}_+^a)_{21} (\mathbf{R}_-^a)_{12}) \\ & + \mu_2^a \left\{ \left| (\mathbf{R}_+^a)_{13} (\mathbf{R}_-^a)_{31} \right| + \sum_{k=1}^2 (\mathbf{R}_+^a)_{1k} (\mathbf{R}_-^a)_{k1} \right\} + \left\{ \left| (\mathbf{R}_+^a)_{23} (\mathbf{R}_-^a)_{32} \right| + \sum_{k=1}^2 (\mathbf{R}_+^a)_{2k} (\mathbf{R}_-^a)_{k2} \right\}. \end{aligned} \quad (28)$$

The above inequality may seem tedious, but it can be straightforwardly proved by expanding all the summations and using the relation: $\mu_2^a |(\mathbf{R}_-^a)_{i3} (\mathbf{R}_+^a)_{3i}| \geq |\mu_3^a| |(\mathbf{R}_-^a)_{i3} (\mathbf{R}_+^a)_{3i}|$ for $i = 1, 2$. The two square brackets in the second line of eq. (28) can be identified as $(\mathbf{R}_+^a \mathbf{R}_-^a)_{ii}$ if $(\mathbf{R}_-^a)_{i3} (\mathbf{R}_+^a)_{3i} \geq 0$, or $(\mathbf{R}_+^a \text{diag}(1, 1, -1) \mathbf{R}_-^a)_{ii}$ if $(\mathbf{R}_-^a)_{i3} (\mathbf{R}_+^a)_{3i} < 0$. In either case, we can substitute the second line of eq. (28) with $2\mu_2^a$, since $1 \geq (\mathbf{R}_+^a \mathbf{R}_-^a)_{ii}$ and $1 \geq (\mathbf{R}_+^a \text{diag}(1, 1, -1) \mathbf{R}_-^a)_{ii}$ due to the fact that the matrix elements of the $O(N)$ rotation group cannot be larger than 1. By the same reasoning, we have $1 \geq ((\mathbf{R}_+^a)_{11} (\mathbf{R}_-^a)_{11} + (\mathbf{R}_+^a)_{21} (\mathbf{R}_-^a)_{12})$, and replace the right-hand side of eq. (28) by $\mu_1^a + \mu_2^a$. Summing over the index a , we find $\bar{\mu}_1 + \bar{\mu}_2 \geq \mu_1 + \mu_2$. Together with $\bar{\mu}_1 \geq \mu_1$, we arrive at the desired inequality: $\bar{\mu}_1^2 + \bar{\mu}_2^2 \geq \mu_1^2 + \mu_2^2$.

FULL EXPRESSION OF DENSITY MATRIX FOR SPIN-1 DECAYS

The P-violating effects in $e^+ e^- \rightarrow V$ production, which influence the polarization sum of V , can be parameterized by a term proportional to d_J : $\tilde{\rho}_{ij} = \delta_{ij}/3 - id_J \epsilon_{ijk} \hat{p}^k - (\hat{p}^i \hat{p}^j - \delta^{ij}/3)/2$. When d_J is nonzero, the corresponding

density matrix is given by:

$$\begin{aligned}
\bar{B}^\pm &= \frac{1}{N} \sqrt{1 - y_m^2} \left(y_m c_\theta \hat{p} + (1 + (1 - y_m) c_\theta^2) \hat{k} \right) \text{Re} \left(\frac{F_A}{F_V} \right) \\
&\quad + \frac{d_J}{N} \left(2y_m \hat{p} + 2(1 - y_m) c_\theta \hat{k} + 2y_m d_J \sqrt{1 - y_m^2} s_\theta \text{Im} \left(\frac{F_A}{F_V} \right) \hat{n} + 2c_\theta (1 - y_m^2) \left| \frac{F_A}{F_V} \right|^2 \hat{k} \right), \\
C_{ij} &= \frac{1}{N} \left[\frac{1}{3} \bar{N} \delta_{ij} + (1 - (1 - y_m^2) \left| \frac{F_A}{F_V} \right|^2) (\hat{p}_i \hat{p}_j - \frac{1}{3} \delta_{ij}) - ((1 - y_m) c_\theta (1 - (1 + y_m) \left| \frac{F_A}{F_V} \right|^2)) (\hat{p}_i \hat{k}_j + \hat{k}_i \hat{p}_j - \frac{2}{3} c_\theta \delta_{ij}) \right. \\
&\quad \left. + (1 - y_m) (1 + c_\theta^2 (1 - y_m)) (\hat{k}_i \hat{k}_j - \frac{1}{3} \delta_{ij}) + \sqrt{1 - y_m^2} s_\theta \left((\hat{p}_i \hat{n}_j + \hat{n}_i \hat{p}_j) - (1 - y_m) c_\theta (\hat{k}_i \hat{n}_j + \hat{n}_i \hat{k}_j) \right) \text{Im} \left(\frac{F_A}{F_V} \right) \right] \\
&\quad + \frac{d_J}{N} \text{Re} \left(\frac{F_A}{F_V} \right) \left[2y_m \sqrt{1 - y_m^2} \text{Re} \left(\hat{p}_i \hat{k}_j + \hat{k}_i \hat{p}_j - \frac{2}{3} c_\theta \delta_{ij} \right) + 4(1 - y_m) \sqrt{1 - y_m^2} c_\theta \left(\hat{k}_i \hat{k}_j - \frac{1}{3} \delta_{ij} \right) \right] \\
\bar{N} &= \frac{1}{2} \left[1 + c_\theta^2 + y_m^2 s_\theta^2 + (1 - y_m^2) (1 + c_\theta^2) \left| \frac{F_A}{F_V} \right|^2 \right] + 4d_J \sqrt{1 - y_m^2} c_\theta \text{Re} \left(\frac{F_A}{F_V} \right). \tag{29}
\end{aligned}$$

For an on-shell Z , both the P-conserving and P-violating interactions are dominated by the e^+e^- interaction with the Z boson, and $d_J = -(1 - 4 \sin^2 \theta_W)/(2 - 8 \sin^2 \theta_W + 16 \sin^4 \theta_W)$. For $V = J/\psi$, the P-conserving interaction arises from photon exchange at $\sqrt{s} = m_{J/\psi}$, while the P-violating interaction is again from Z exchange, which gives $d_J = \sqrt{2} m_{J/\psi}^2 G_F (3 - 8 \sin^2 \theta_W)/(32\pi\alpha_{EM})$.

ON EXTRACTING C_{ij} IN EXPERIMENTS

Consider the cascade decays of $i \rightarrow f(\rightarrow f'X)\bar{f}(\rightarrow \bar{f}'X)$, where f' is a spin-1/2 fermion and X represents the rest of the particles. The 3-momenta of f' and \bar{f}' are denoted as \hat{a} and \hat{b} in the rest frames of f and \bar{f} , respectively. The differential distributions are related to the density matrix as

$$\frac{\partial}{\partial c_\theta} \left(\frac{\partial^4 N}{\partial \phi_i^a \partial \hat{a}_i \partial \phi_j^b \partial \hat{b}_j} \right) = \frac{1}{16\pi^2} \frac{\partial N}{\partial c_\theta} \left(1 + \alpha' \bar{B}^+ \cdot \hat{a} + \bar{\alpha}' \bar{B}^- \cdot \hat{b} + \alpha' \bar{\alpha}' (\hat{a} \cdot \mathbf{C} \cdot \hat{b}) \right), \tag{30}$$

where $i, j = x, y, z$, N stands for the number of observed events, and α' ($\bar{\alpha}'$) is the polarization fraction of f' (\bar{f}') in $f \rightarrow f'X$ ($\bar{f} \rightarrow \bar{f}'X$). Here, ϕ_i^a and ϕ_j^b represent the azimuthal angles of \hat{a} and \hat{b} about i and j , respectively.

Explicitly, for $i = z$, we have

$$(\hat{a}_x, \hat{a}_y, \hat{a}_z) = (\cos \phi_z^a \sin \theta_z^a, \sin \phi_z^a \sin \theta_z^a, \cos \theta_z^a) \tag{31}$$

and $d\phi_z^a d\cos \theta_z^a$ corresponds to the differential surface area expanded on a unit sphere. On the other hand, if we choose $i = x$ or $i = y$ instead, we replace $(\hat{a}_x, \hat{a}_y, \hat{a}_z)$ in eq. (31) by $(\hat{a}_y, \hat{a}_z, \hat{a}_x)$ or $(\hat{a}_z, \hat{a}_x, \hat{a}_y)$, while replacing (θ_z^a, ϕ_z^a) with (θ_x^a, ϕ_x^a) or (θ_y^a, ϕ_y^a) . The same arguments apply to \hat{b} . The choice of i and j does not affect the expression on the right-hand side of eq. (31) due to the unity of the Jacobian. To extract C_{ij} , we integrate over ϕ_i^a and ϕ_j^b and find

$$\frac{\partial}{\partial c_\theta} \left(\frac{\partial^2 N}{\partial \hat{a}_i \partial \hat{b}_j} \right) = \frac{1}{4} \frac{\partial N}{\partial c_\theta} (1 + \alpha' B_i^+ \cos \theta_i^a + \bar{\alpha}' B_i^- \cos \theta_j^b + \alpha' \bar{\alpha}' \cos \theta_i^a \cos \theta_j^b C_{ij}). \tag{32}$$

We do not sum over i and j . The integration over a bin of c_θ , \hat{a}_i , and \hat{b}_j on the left-hand side of Eq. (32) can be obtained from experiments. There are many ways to extract B_i^\pm and C_{ij} . We provide the simplest two-bin scenario:

$$\bar{C}_{ij} = \frac{4}{N_{\omega_1}^{\omega_2}} \int_{\omega_1}^{\omega_2} dc_\theta \left(\int_0^1 d\cos \theta_i^a - \int_{-1}^0 d\cos \theta_i^a \right) \left(\int_0^1 d\cos \theta_j^b - \int_{-1}^0 d\cos \theta_j^b \right) \frac{\partial}{\partial c_\theta} \left(\frac{\partial^2 N}{\partial \hat{a}_i \partial \hat{b}_j} \right). \tag{33}$$

Here, $N_{\omega_1}^{\omega_2}$ is the total number of observed events in the range $\omega_2 \geq c_\theta \geq \omega_1$, and \bar{C}_{ij} is the average spin-correlation matrix element over the same range. For spin-0 decays, C_{ij} does not depend on c_θ , and we have $\bar{C}_{ij} = C_{ij}$. For $\Lambda_b^0 \rightarrow \Lambda_c^+ \pi^-$, $\Lambda_c^+ \rightarrow \Lambda \pi^+$ and $\tau^- \rightarrow \nu_\tau \pi^-$, CP is conserved in the cascade decays and we have $\alpha' = -\bar{\alpha}'$. Numerically, they are found to be $\alpha' = -1.003 \pm 0.008 \pm 0.005$, $\alpha' = -0.785 \pm 0.007$ and $\alpha' = -1$, respectively [29].